



**IJMRBS**

ISSN: 2319-345X

# **International Journal of Management Research and Business Strategy**

[www.ijmrbs.org](http://www.ijmrbs.org)



**E-mail**

[editor@ijmrbs.org](mailto:editor@ijmrbs.org)

[editor.ijmrbs@gmail.com](mailto:editor.ijmrbs@gmail.com)

# A FLEXIBLE HYDROFOIL PROPELLER SIMULTANEOUSLY LIKE A FISH

Mogulappa<sup>1</sup>, Etikala Sainath<sup>2</sup>, G. Anitha<sup>3</sup>,  
Assistant Professor<sup>1,2</sup>,  
Student<sup>3</sup>,

Department of Mechanical,  
BRILLIANT GRAMMAR SCHOOL EDUCATIONAL SOCIETY'S GROUP OF INSTITUTIONS-  
INTEGRATED CAMPUS  
Abdullapurmet (V), Abdullapurmet (M), R.R Dt. Hyderabad-501505.

## Article Info

Received: 09-09-2022

Revised: 01-10-2022

Accepted: 25-11-2022

## ABSTRACT

The exceptional hydrodynamic qualities of the hydrofoil have made it a popular choice for underwater vehicles. Rigid hydrofoil research is well-established at this time, but flexible hydrofoils, such as the caudal fin, have not yet been given the attention they deserve. The fish was considered the bionic item in this study. Then, the kinematics model was proposed to account for the fish's swimming motion. To replicate this sine curve motion while swimming, a fin-peduncle propulsion system was developed using a kinematics model. Matlab was used to optimize the propulsion mechanism, which allowed for a less discrepancy between the actual motion trajectory and the fin-peduncle propulsion mechanism's output curve. Moreover, the motion phase angles of the movable articulations are tuned to lessen the drag and increase the effectiveness of the propulsion system. Lastly, a fluid-solid coupling approach based on Fluent is used to model the fish-like oscillation of a hydrofoil. It was shown that a flexible oscillation comparable to that of a fish may be tuned to produce a motion that adheres to the same law of sine. Oscillating hydrofoil propellers have a substantially better propulsive efficiency than screw propellers, and the flexible oscillation has a higher propulsive efficiency than the stiff oscillation without obviously increasing the fluid resistance. **Keywords:** bionics; flexible hydrofoil; phase angle; hydrodynamic coefficient

## INTRODUCTION

The Autonomous Underwater Vehicle (AUV) has proven to be an invaluable tool for maritime tasks such as underwater pipeline installation and equipment maintenance. Over many millions of years, marine life has contributed to natural progression. Incorporating bionics into AUV research will be a huge help. Fish had excellent underwater speed and maneuverability. The dolphin's turning radius may be 23% to 30% of its Body length and it can swim at speeds of 3 to 7 times its own length per second [1]. In 1994, Robo Tuna, the first fish-like robot, was created at MIT, and it could swim at a top speed of 2 meters per second [2]. Since then, the fish-like robot has received even more media attention. The Japanese developed the PF-300 [3], a fish-shaped robot powered by a pair of motors that work together to move the robot's body. The robotic bluefin tuna [4] was created by engineers at Harbin Engineering University to look like the real thing, complete with a three-link tail. With a flexible body and propulsion efficiency of up to 65% [5], Du Ruxu's robot fish is a technological marvel. Fish-like robots called SPC were created by researchers at Beihang University, and they've swum as far as 70.2 kilometers [6]. There have also been several numerical investigations of the hydrodynamic properties of an oscillating hydrofoil. For the deformable body, the slender-body hypothesis was proposed to characterize the circumstances under which fish may benefit from increased Froude propulsion efficiency [7]. To investigate all.

research, the time-dependent turbulent flows around a Clark-Y hydrofoil were elucidated by using Lagrangian coherent structures (LCS) described by the ridges of the finite-time Lyapunov exponent (FTLE) [9].

The flexible oscillating hydrofoil propeller, which resembles a fish fin, outperforms the screw propeller in terms of both propulsion efficiency and responsiveness. The fin-peduncle propulsion system was developed and refined in this study to mimic the swimming of fish. Moreover, the phase angles of the various movable articulations are tuned to lessen the drag and increase the effectiveness of the propulsion system. Lastly, a fluid-solid coupling approach using Fluent is used to model the fish-like oscillation of a hydrofoil.

## PROPULSION MECHANISM

### KINEMATICS MODEL

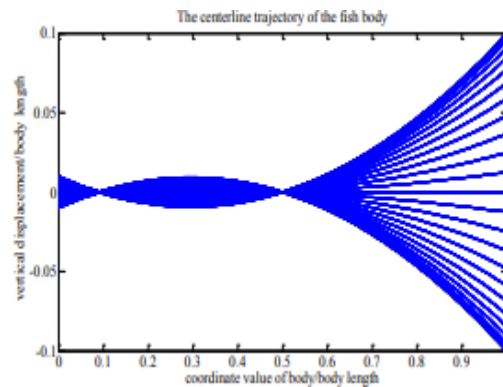
According to the observation of fish swimming, an equation to describe the centerline trajectory of the swimming fish body was put forward [10].

$$h(x_n, t) = H(0.21 - 0.66x_n + 1.1x_n^2 + 0.35x_n^3) \sin(2\pi ft) \quad (1)$$

Where  $x_n$  is the ratio of the body coordinate value (marked as  $x$ ) and the body length (marked as  $L$ ),  $t$  is the movement time,  $h(x_n, t)$  is the oscillation amplitude of the body,  $H$  is the maximum oscillation amplitude at the end of the caudal peduncle,  $f$  is the oscillating frequency of the caudal peduncle. After studying the oscillating movements of the fish body, Wang simplified the kinematics model [11]. Supposing that the maximum oscillation amplitude of the fish head is one tenth of the body length and the oscillation amplitude of the barycenter is zero, the simplified equation for the centerline trajectory of the fish body can be described as:

$$h(x_n, t) = H(0.1 - 1.3x_n + 2.2x_n^2) \sin(2\pi ft) \quad (2)$$

The centerline trajectories of the fish body at different moment are shown in Fig. 1.



The kinematics equation at the end of the tail can be described as:

$$h(t) = H \sin(2\pi ft) \quad (3)$$

The pitching movement of the caudal fin lags behind its plunging movement, which can be described as:

$$\theta(t) = \theta_{\max} \sin(2\pi ft + \phi) \quad (4)$$

where  $\theta_{\max}$  is the maximum oscillation angle, and  $\phi$

is the phase angle between the plunging movement and the pitching movement.

The swimming speed of the fish can be marked as  $v$  and the length of the caudal fin can be marked as  $l$ . The kinetic coordinate system for caudal fin can be established, as shown in Fig. 2.

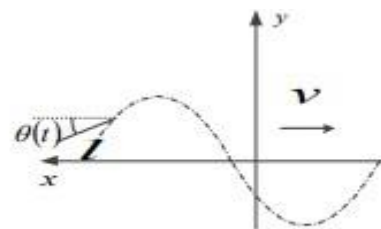


Fig. 2 The kinetic coordinate system for caudal fin

In Fig. 2, the full line is the caudal fin and the dotted line is the plunging movement trajectory of the caudal fin. The coordinate value for the movement of the caudal fin at any time in the kinetic coordinate can be described as:

$$x = vt - l \cos[\theta_{\max} \sin(2\pi ft + \varphi)] \quad (5)$$

$$y = H \sin(2\pi ft) - l \sin[\theta_{\max} \sin(2\pi ft + \varphi)] \quad (6)$$

$$l_3 \sin \beta + l_4 \cos \alpha = l \quad (7)$$

$$x_C = l_1 \cos \theta \quad (8)$$

$$x_D = l_1 \cos \theta + l_2 \quad (9)$$

$$x_E = l_1 \cos \theta + l_2 + l_3 \cos \beta \quad (10)$$

$$x_F = l_1 \cos \theta + l_2 + l_3 \cos \beta + l_4 \sin \alpha \quad (11)$$

$$l_1 \cos \theta + l_2 + \sqrt{l_3^2 - (l - l_4 \cos \alpha)^2} + l_4 \sin \alpha = L \quad (12)$$

## MECHANISM DESIGN

The propulsion mechanism for the fish-like flexible oscillating hydrofoil propeller was designed based on the kinematics model. The mechanism sketch is shown in Fig. 3.

As shown in Fig. 3, member AB, rotating around A, is driven by the servo motor. The rotation is transformed into the sinusoidal reciprocating motion of member CD, which is connected with member AB by prismatic joint and revolute joint. Member CD and member EF are connected to member DE by revolute joints. Member EF is fixed to member FG. Member CD will drive member DE, member EF, and member FG to achieve the sinusoidal movement output. An actuator is fixed at the end of member FG to control the caudal fin swinging lagged behind member FG in certain phase angle independently.

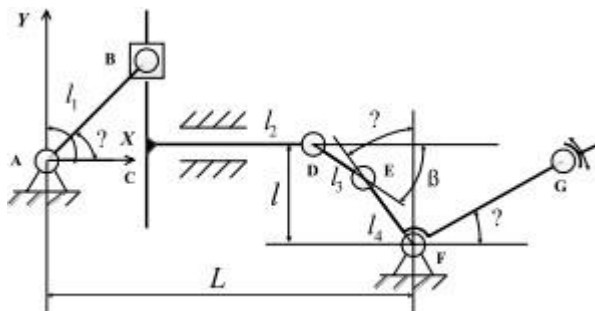


Fig. 3 The mechanism sketch of the propulsion mechanism

In Fig. 3, a coordinate system is established where the origin is point A. Point F is fixed on the coordinate. As the position relations shown in Fig. 3, some formulas can be deduced as:

where  $C_x$ ,  $D_x$ ,  $E_x$ , and  $F_x$  are the coordinate values of C, D, E, and F.  $l_1$ ,  $l_2$ ,  $l_3$ , and  $l_4$  are the length of member AB, member CD, member DE, and member EF.  $l$  is the distance between point D and point F in Y direction.  $L$  is the distance between point A and point F in X direction.  $\alpha$ ,  $\beta$ , and  $\theta$  are the angles as shown in Fig. 3. The propeller model was designed based on the mechanism sketch, as shown in Fig. 4.

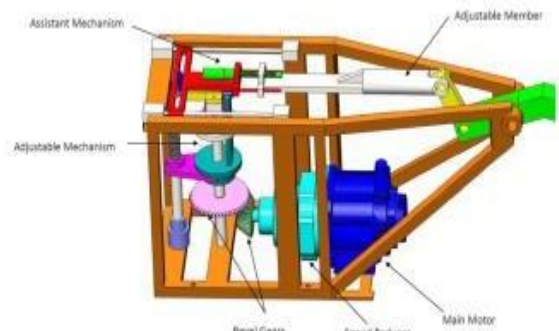


Fig. 4 The propeller model

The length of the adjustable member can be changed. If the adjustable member is shortened, the balanced position for the plunging movement of caudal peduncle will move up, and if the adjustable member is lengthened, it will move down. So the swimming direction of the fish-like robot will be controlled by the adjustment of the adjustable member length.



## OPTIMIZATION BASED ON MATLAB

The length of the mechanism members affects the plunging movement of caudal peduncle, which increases the difficulty of the propulsion mechanism design. At present, the most used method for the mechanism design with the given motion law or the motion trajectory is the function approximation method [12]. However, it is very complicated for the multivariable mechanism optimization. Matlab contains a variety of optimization toolbox, which can be applied in the design optimization of the mechanism to improve the efficiency and accuracy of the calculation.

The propulsion mechanism can be simplified as Fig. 5 shown.

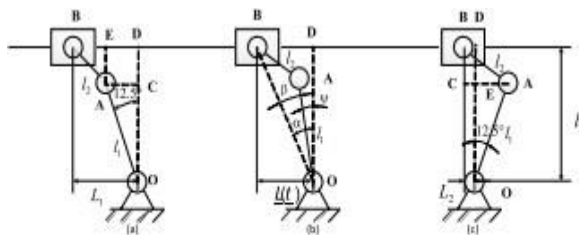


Fig. 5 Mechanism Moment Position

The left limit position is shown in position (a), the right limit position is shown in position (c), and position (b) shows any moment position of the movement. The block B goes the sinusoidal reciprocating motion.

The oscillating frequency of the plunging movement is about 2.1Hz and the range of that is about 25° according to the observation. It means the oscillating range of member OA is about 12.5°. The length of member OA (marked as  $l_1$ ), the length of member AB (marked as  $l_2$ ), the vertical height between point B and point O (marked as  $3l$ ), and the movement stroke of block B (marked as  $L$ ) are the main parameters to affect the final output of the mechanism.  $l_1$ ,  $l_2$ , and  $3l$  are the design variables and the follow equation can be established as:

$$x = [l_1; l_2; l_3]^T \quad (13)$$

As shown in Fig. 5(b), the horizontal distance between point B and point O can be described by  $L(t)$ , as:

$$L(t) = 0.5L \cos 4\pi t + \frac{L_1 + L_2}{2} \quad (14)$$

Where  $t$  is the movement time,  $L_1$  and  $L_2$  are the horizontal distance of the left limit position and the right position between point B and point O.

As shown in Fig. 5(a) and Fig. 5 (c),  $L_1$  and  $L_2$  can be described as:

$$L_1 = \sqrt{l_2^2 - (l_3 - l_1 \cos 12.5^\circ)^2} + l_1 \sin 12.5^\circ \quad (15)$$

$$L_2 = \sqrt{l_2^2 - (l_3 - l_1 \cos 12.5^\circ)^2} - l_1 \sin 12.5^\circ \quad (16)$$

The ideal oscillating law of member OA can be described by  $\Psi$ , as:

$$\Psi = 12.5^\circ \sin 4\pi t \quad (17)$$

To minimize the square of the difference between the mechanism output angle and the ideal output angle, the target function can be described as:

$$F(x) = \sum_{t=0}^{0.25} [\Psi(x) - \Psi]^2 \quad (18)$$

$$\Psi(x) = \alpha(t) - \beta(t) \quad (19)$$

where  $\alpha(t)$  and  $\beta(t)$  can be calculated from  $\triangle OBD$  and  $\triangle OAB$  as:

$$\alpha(t) = \arccos \left[ \frac{l_3}{\sqrt{l_3^2 + L^2(t)}} \right] \quad (20)$$

$$\beta(t) = \arccos \left\{ \frac{l_1^2 + [l_3^2 + L^2(t)] - l_2^2}{2l_1 \sqrt{l_3^2 + L^2(t)}} \right\} \quad (21)$$

The swimming resistance is little with the streamlined shape. It is shown that the swimming resistance will reduce 75% with the slender ratio of the fish body being 4.5 under the bionics theory. In

this research, the length of the fish-like robot body was set as 0.9m, so the widest of the body is no more than 0.2m. Besides, in order to make the robot swim autonomously, the swimming parameters should be variable according to different conditions, so the movement stroke of block B cannot be too small.

To achieve the good transmission of the mechanism, the minimum transmission angle should be larger than  $40^\circ$ . The two limit positions of the movement are shown in Fig. 6. The transmission angle at the limit position should be larger than  $40^\circ$ , which will make sure the good transmission at any time of the movement.

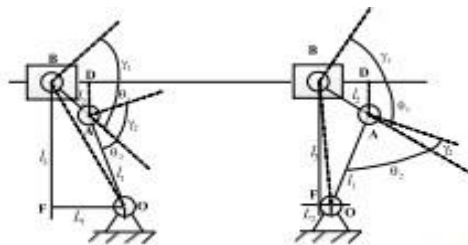


Fig. 6 The transmission angle at the limit position  $\theta_1$

In Fig. 6, the constraint conditions of the pressure angle at the limit position can be obtained from  $\triangle ADB$ , as:

$$\frac{l_3 - l_1 \cos 12.5^\circ}{l_2} \leq \sin 50^\circ \quad (22)$$

In Fig. 6, the constraint conditions of the pressure angle  $\theta_2$  at the limit position can be obtained from  $\triangle OAB$ , as:

$$\frac{l_1^2 + l_3^2 - l_2^2 - l_2^2}{2l_1l_2} \geq \cos 50^\circ \quad (23)$$

$$\frac{l_2^2 + l_3^2 - l_1^2 - l_2^2}{2l_1l_2} \geq \cos 50^\circ \quad (24)$$

The optimization of rod mechanism is simple nonlinear programming problem, and the fmincon function in Matlab toolbox is available. Therefore, the target function was calculated every 0.02s and all the results were accumulated to a sum. According to the optimization, the optimal design variables of the solution are

$[143.605; 62.196; 187.8459]T$  mm, which means  $l_1$  mm = 143.605,  $l_2$  mm = 62.196, and  $l_3$  mm = 187.8459. The lengths are set as  $l_1$  mm = 144,  $l_2$  mm = 62, and  $l_3$  mm = 188 for manufacturing and the output angle of the mechanism is compared with the ideal output angle, as shown in Fig. 7.

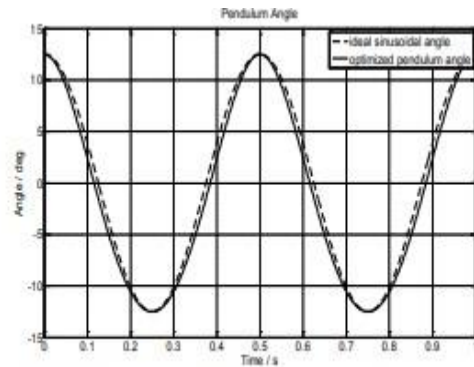


Fig. 7 The output angle of the mechanism and the ideal output angle

In Fig. 7, the dotted line is the ideal outputs angle and the solid line is the actual output angle of the designed mechanism. It comes to the conclusion that the actual output angle amplitude of the designed propulsion mechanism is  $12.5^\circ$  and changes follow the similar law of sine, which is similar to the ideal output angle.

## STUDY OF PHASE ANGLE

The forces on the caudal fin were analysed, as shown in Figure 8.

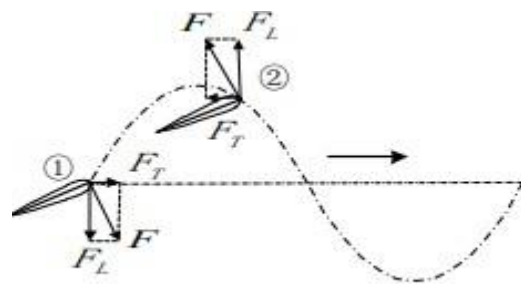


Fig. 8 Analysis of the forces on caudal fin

In Fig. 8,  $F_T$  is the thrust force, which goes along the forward direction at position ①, and it is positive. The caudal fin moves down with the caudal peduncle at position ②, and the force direction is perpendicular to the caudal fin upward. The thrust force goes along the reverse-forward direction, which is negative.

As the observation of the fish swimming, the relation between the swimming velocity and the oscillating frequency is linear. Besides, the oscillation amplitude of the caudal peduncle is essentially unchanged during the swimming process. The biologists point out that the amplitude of the caudal peduncle oscillation is about 0.17 to 0.25 times of the body length. Therefore, the movement parameters of the fish-like robot are as follows:

Swimming speed:  $v$  Lm / s ;

Maximum oscillation range of the caudal fin:  $H$  Lm  
 $= 0.1$  ; Frequency of the oscillation:  $f$  Hz = 2 ;  
 Maximum oscillation angel range of the caudal fin:

$$\theta_{\max} = 30^{\circ}.$$

The phase differences between the pitching movement of caudal fin and the plunging movement of caudal peduncle are set as  $60^{\circ}$ ,  $90^{\circ}$  and  $120^{\circ}$  for the kinematics simulation. The oscillation of the caudal fin and the motion trajectory of the swing shaft are shown in Fig. 9 to Fig. 11

As the phase difference is  $60^{\circ}$ , the caudal fin produces more negative force than positive negative force, and it is the same as the phase difference is  $120^{\circ}$ . When the phase difference is  $90^{\circ}$ , the caudal fin produces positive thrust all the period. So it is considered that the phase difference between the caudal fin plunging movement and pitching movement controls the attack angle of the caudal fin movement, and  $90^{\circ}$  is the best phase angel.

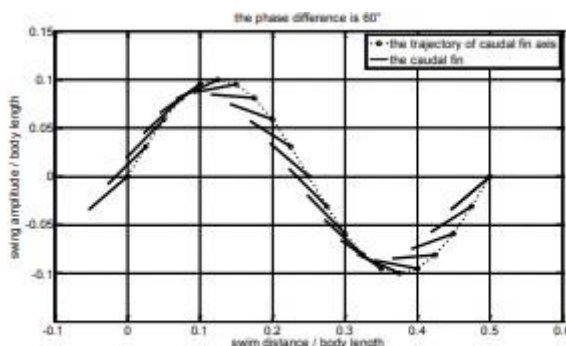


Fig. 9 The phase difference is  $60^{\circ}$

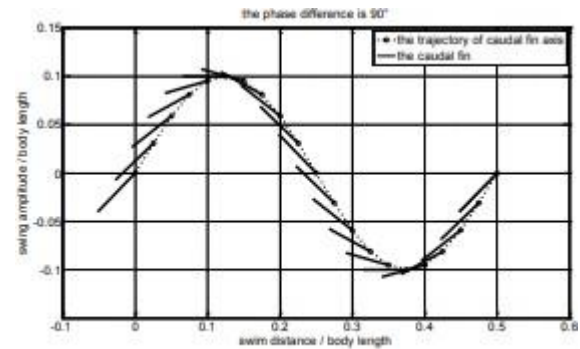


Fig. 10 The phase difference is  $90^{\circ}$

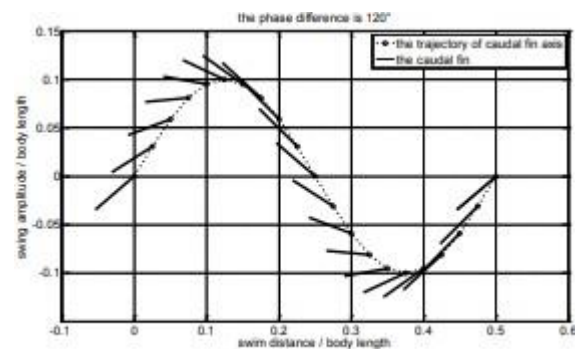


Fig. 11 The phase difference is  $135^{\circ}$

## HYDRODYNAMIC COEFFICIENTS ANALYSIS

The hydrodynamic coefficients can be defined as:

$$c_d = \frac{F_d}{\frac{1}{2} \rho C_0 v^2} \quad (25)$$

$$c_l = \frac{F_l}{\frac{1}{2} \rho C_0 v^2} \quad (26)$$

$$c_m = \frac{M}{\frac{1}{2} \rho C_0^2 v^2} \quad (27)$$

where  $c_d$  is drag coefficient,  $c_l$  is lateral force coefficient,  $c_m$  is moment coefficient,  $F_d$  is drag produced by flexible oscillating hydrofoil,  $F_l$  is lateral force produced by flexible oscillating hydrofoil,  $M$  is oscillation moment around the head of the fish body produced by flexible oscillating

hydrofoil,  $\rho$  is fluid density,  $C_0$  is chord length of the hydrofoil,  $v$  is flow velocity of the fluid.

The SIMPLE Method (Semi-implicit Method for Pressure Linked Equations) was used to solve the pressure-velocity coupling equations, and the UDF (User Defined Function) was used to achieve the flexible oscillation in the commercial software Fluent. In the simulation, the oscillation frequency of the fish body and the caudal fin is 2Hz, the hydrofoil is the airfoil of NACA0014, the chord length of fish body is 200mm, the chord length of caudal fin is 60mm, and the oscillating scope of caudal fin is  $\pm 45^\circ$ .

In the kinematics model,  $H$  is the maximum lateral oscillation amplitude at the end of the fish body, which could express different flexibilities in different values. The flexibility is better with larger lateral oscillation amplitude. If  $H$  is zero, the fish body is rigid without any oscillation, but the caudal fin will oscillate as usual.

The hydrodynamic characteristics of flexible oscillating hydrofoil were analysed in the still water under the condition that the fish oscillated in situ. To use the commercial software Fluent, a minor water flow velocity should be available. The flow velocity was set as 0.01m/s to avoid distinct influence on the flow field.

The curves of the drag coefficient and the lateral force coefficient of fish body in a period in the still water with different oscillation amplitude are shown in Fig. 12

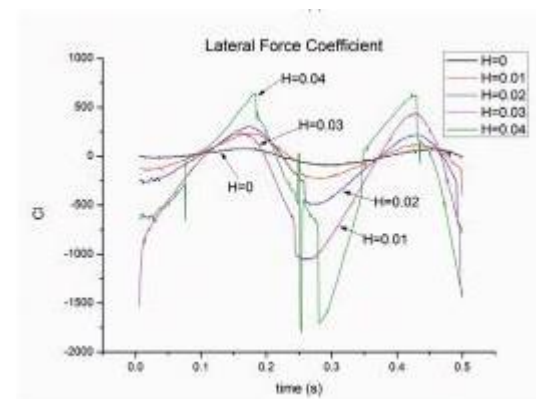
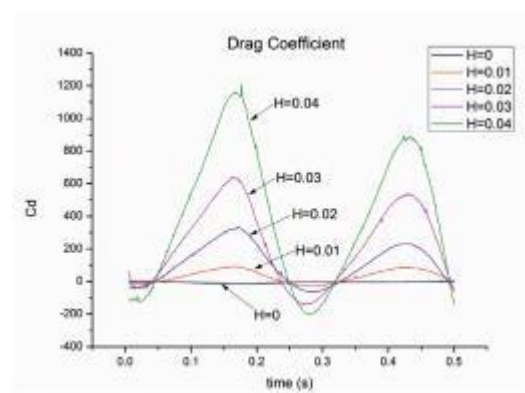


Fig. 12 Drag coefficient curves and lateral force coefficient curves of fish body in the still water

The drag coefficient curves indicate that the drag coefficient approximates a straight line when the fish body doesn't oscillate ( $H = 0$ ), which means the fish body produce no thrust force. The amplitude of the drag coefficient increases with the flexible oscillating amplitude of the fish body getting larger. There are two peak values in a fish body oscillation period and the drag coefficient variation period is half of the fish body oscillation period. The maximum values appear at the 1/4 period and 3/4 period of the fish body oscillation, which means the fish body produces the maximum thrust at these two moments. The integration value during the whole period is positive, which indicates that the fish could go forward with the fish body oscillation in the still water.

As shown in the lateral force coefficient curves, the amplitude and fluctuation of the lateral force increase with the flexibility getting better, and the lateral force generated by the oscillation is unstable. At the 1/2 period of the oscillation, the immense change occurs because the fish body oscillates from one side of the center line to another side. The lateral force consumes the energy generated by the oscillation and increases the swimming instability.

The curves of the drag coefficient and the lateral force coefficient of caudal fin during an oscillation period in the still water with different oscillation amplitude are shown in Fig. 13.



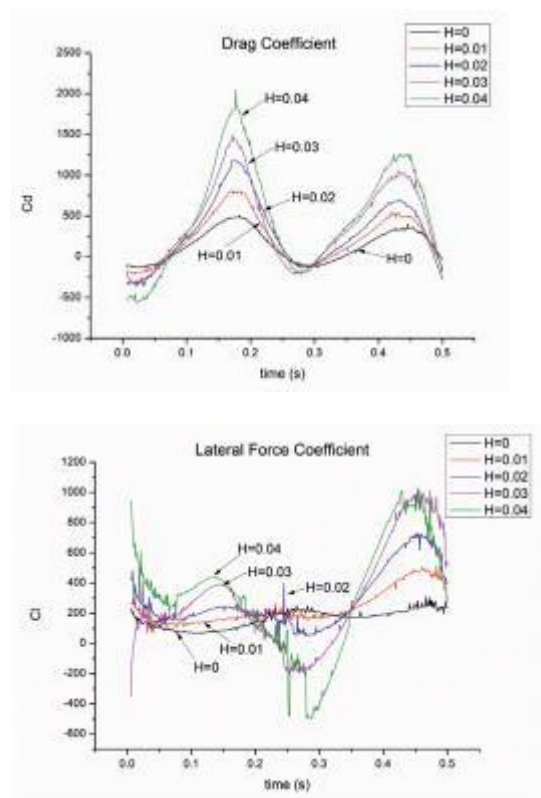


Fig. 13 Drag coefficient curves and lateral force coefficient curves of caudal fin in the still water

As shown in drag coefficient curves, the change trend of the drag coefficient produced by the caudal fin oscillation is same as that of the fish body oscillation. The amplitude of the caudal fin drag coefficient increases with the flexibility and the oscillation amplitude of the fish body getting larger. The comparison between the drag coefficient curves of fish body and caudal fin shows that the drag coefficient value of the caudal fin is bigger, which means that the wake field generated by the fish body oscillation promotes the drag coefficient produced by the caudal fin compared with the oscillation without wake field. The drag coefficient values are almost positive in the whole period, which means the oscillation of the caudal fin has evident effects on the propulsion.

As shown in lateral force coefficient curves, the lateral force generated by the caudal fin oscillation increases with the flexibility and oscillation amplitude of the fish body getting larger under the same angle oscillation amplitude of the caudal fin, which indicates that more energy generated by the caudal fin oscillation is consumed. Most of the

lateral force coefficient values are positive and the integration during an oscillation period is not equal to zero, which indicates that the caudal fin oscillation would accumulate to unidirectional force and go against the swimming. Accordingly, the unidirectional force should be reduced with the actuator controlling the amplitude and phase of the caudal fin oscillation in the fishlike robot development.

## CONCLUSION

Using this study, we were able to construct a kinematics model for the swimming behavior of the robot fish and use it to inform the development of its propulsion system. Matlab's `fmincon` function was used to determine the optimum length of the propulsion mechanism's parts. It is shown that the motion curves produced by the fin-peduncle propulsion system are quite close to the ideal motion.

Scientists looked at the lag time between the caudal fin's pitching and the caudal peduncle's diving movements. If the phase angle were 90 degrees, the thrust mechanism would generate thrust during the whole period of motion. In contrast to the single, swaying caudal fin, the benefits of the articulatory fin-peduncle system are readily apparent.

The drag coefficient, lateral force coefficient, and moment coefficient all have fluctuation periods that are half that of the oscillation period of the fish body, whereas the period of variation of the moment coefficient is the same as that of the oscillation period. In calm water, the amount of energy used is proportional to the amplitude of the flexible oscillations, which is why a greater amplitude results in a larger lateral force integration value in a given time period.

## CONFLICT OF INTEREST

The authors declared that they have no conflicts of interest to this work

## ACKNOWLEDGEMENTS

The research was supported by the front and emerging discipline team oriented project of

Shandong University “marine resources and utilization of key scientific research”

(project number 2014QY006) and “The Fundamental Research Funds of Shandong University” (2016JC035), hereby thanks.

## References

1. Nagai, M. (2002). Thinking fluid dynamics with dolphins. US: IOS Press.
2. Triantafyllou, M. S., and Triantafyllou, G. S. (1995). An efficient swimming machine. *Scientific American*, 272(3): 64-70.
3. Koichi, H., Tadanori, T., and Kenkichi, T., 2000, “Study on turning performance of a fish robot,” First International Symposium on Aqua Bio-Mechanisms, pp. 287-292.
4. Cheng, W., 2004, “Research on Simulation and Control Technology for Bionic Underwater Vehicle,” Ph.D. thesis, Harbin Engineering University, Harbin, China.
5. Du, R. X., Li, Z., Kamal, Y. T., Pablo, V. A., 2015, “Robot Fish,” New York: Springer Tracts in Mechanical Engineering.
6. Liang, J. H., Zhang, W. F., Wen, L., Wang, T. M., Liu, and Y. J. (2010). Propulsion and Maneuvering Performances of Two-Joint Biorobotic Autonomous Underwater Vehicle SPC-III. *Robot*, 32(6):726-731.
7. Lighthill, M. J. (1960), Note on the swimming of slender fish, *Journal of Fluid Mechanics*, Vol.9: 305-317.
8. Leroyer, A., Visonneau, M.(2005), Numerical methods for RANSE simulations of a self-propelled fish-like body, *Journal of Fluids and Structures*, Vol.20, No.7: 975-991.
9. Zhao, Y., Wang G. Y., Huang, B., Wu, Q., Wang, F. F. (2015), Lagrangian-Based Investigation of Unsteady Vortex Structure Near Trailing Edge of a Hydrofoil, *Transactions of Beijing Institute of Technology*, Vol.35, No.7: 666- 670.
10. Romanenko, E. V. (2002). Fish and dolphin swimming. Bulgaria: Pensoft Publishers.
11. Wang, L., Yu, J. Z., Hu, Y. H., Fan, R. F., Huo, J. Y., and Xie, G. M. (2006). Mechanism design and motion control of robotic dolphin. *Acta Scientiarum Naturalium Universitatis Pekinensis*, 42(3): 294-301.
12. Wang, W. J. (2006). Optimal design of planar linkage based on Matlab optimization toolbox. *Light Industry Machinery*, 24(4): 76